Cell Biol Toxicol (2025) 41:96
https://doi.org/10.1007/s10565-025-10049-z

RESEARCH

Loss of YTHDF1 suppresses the progression of malignant rhabdoid tumor of the kidney by regulating Glutathione S-transferase Mu 2 (GSTM2)

Qian-Wen Xiong · Yuntao Liu · Min He · Xiao-Die Shen · Manli Zhao · Shuang-Ai Liu · Gensheng Zhang · Qian Liu · Jinhu Wang · Wan-Xin Peng

Received: 15 October 2024 / Accepted: 30 May 2025

Abstract

Background Malignant rhabdoid tumor of the kidney (MRTK) is a rare renal tumor with poor prognosis. While germline mutations of *SMARCB1* are considered to be the primary cause of MRTK, emerging evidence suggests that somatic epigenetic changes also play a vital role in the development and progression of MRTK. YTHDF1, an m6A reader protein, has been implicated in regulation of tumorigenesis by influencing RNA translation and stability in several adult cancers. However, the exploration of the role of YTHDF1 in pediatric cancer, especially MRTK, remains limited.

Methods In this study, CRISPR/Cas9 was employed to knockout (KO) YTHDF1 in G401 cells. The impact of YTHDF1 on the cell growth and chemoresistance were assessed using CCK-8 assays. Western blot and qRT-PCR were used to determine the changes in ferroptosis marker gene expression. Additionally, 4D-label free quantitative proteomics was conducted to uncover alterations by YTHDF1 deletion.

Results We observed that the deletion of YTHDF1 in the MRTK cell line led to a significant reduction in malignancy-associated characteristics, including decreased cell motility, invasive growth, and chemoresistance. Quantitative proteomic analysis revealed

Qian-Wen Xiong, Yuntao Liu and Min He contributed equally to this work.

Supplementary Information The online version contains supplementary material available at https://doi.org/10.1007/s10565-025-10049-z.

Q.-W. Xiong · M. He · X.-D. Shen · S.-A. Liu · J. Wang (✉)
Department of Surgical Oncology, National Clinical Research Center for Child Health, National Children's Regional Medical Center, Children's Hospital, Zhejiang University School of Medicine, Hangzhou, China
e-mail: wjh@zju.edu.cn

Q.-W. Xiong · W.-X. Peng (✉)
Hangzhou TCM Hospital Affiliated to Zhejiang Chinese Medical University (Hangzhou Hospital of Traditional Chinese Medicine), Hangzhou, China
e-mail: pengwanxin@gmail.com

Y. Liu
Institute of Neuroscience, Basic Medicine College of Chongqing Medical University, Chongqing, China

M. Zhao
Department of Pathology, National Clinical Research Center for Child Health, National Children's Regional Medical Center, Children's Hospital, Zhejiang University School of Medicine, Hangzhou, China

G. Zhang
Department of Nephrology, National Clinical Research Center for Child Health, National Children's Regional Medical Center, Children's Hospital, Zhejiang University School of Medicine, Hangzhou, China

Q. Liu
School of Basic Medical Science, Chongqing University of Chinese Medicine, Chongqing, China

Published online: 07 June 2025

that the glutathione-related signaling pathway was notably affected by YTHDF1 KO. Specifically, YTHDF1 KO resulted in a reduction of both mRNA and protein levels of Glutathione S-Transferase Mu 2 (GSTM2), a phase II metabolizing enzyme responsible for conjugating glutathione to electrophilic compounds. The decrease in GSTM2 levels following YTHDF1 KO increased the susceptibility of MRTK cells to ferroptosis. Notably, overexpression of GSTM2 in YTHDF1 KO cells partially restored the oncogenic phenotype of MRTK cells, underscoring its role in MRTK progression.

Conclusions In summary, our findings provide new insights into the molecular mechanisms driving MRTK progression, highlighting YTHDF1 and GSTM2 as potential therapeutic targets for this aggressive pediatric renal tumor.

Keywords MRTK · YTHDF1 · M6 A · GSTM2 · Ferroptosis

Abbreviations

4D-LFQ	4D-Label-free quantitative proteomics
4-HNE	4-Hydroxynonenal
ALL	Acute myeloid leukemia
DMEM	Dulbecco's Modified Eagle Medium
DHODH	Dihydroorotate dehydrogenase
FBS	Fetal bovine serum
FSP1	Ferroptosis suppressor protein 1
GO	Gene ontology
GPX4	Glutathione peroxidase 4
GSH	Glutathione
GST	Glutathione S-transferase
GSTM2	Glutathione S-transferase Mu 2
HP	Hepatoblastoma
KEGG	Kyoto Encyclopedia of Genes and Genomes
KO	Knockout
m6 A	N6-methyladenosine
MeRIP	M6A RNA immunoprecipitation
MRTK	Malignant rhabdoid tumor of the kidney
MS	Mass spectrometry
NASH	Non-alcoholic steatohepatitis
NB	Neuroblastoma
PCR	Polymerase chain reaction
PRDX1	Peroxiredoxin 1
qRT-PCR	Quantitative RT-PCR
RIP	RNA immunoprecipitation
ROS	Reactive oxygen species
SDS	Sodium dodecyl sulphate
YTHDF1	YTH N6-methyladenosine RNA binding protein 1

Introduction

Malignant rhabdoid tumor of the kidney (MRTK) is a rare and highly aggressive embryonal tumor with a poor prognosis, predominantly affecting pediatric patients. It is known for resistance to both radiotherapy and chemotherapy, contributing to a dismal 5-year overall survival rate of 20–30% (Xie 2023; Voglino et al. 2015; Cheng, et al. 2007; Koh et al. 2023; Liu et al. 2023). While germline mutations in the tumor suppressor gene *SMARCB1* are the primary driver of MRTK in most cases, recent studies suggest that additional genetic and molecular factors contribute to its development and progression (Smith et al. 2014). Further investigation into the molecular pathways dysregulated in MRTK could provide insights into novel therapeutic strategies.

Epigenetic alterations, the well-known hallmark of cancer, are known to regulate the expression of key genes involved in tumorigenesis(Hanahan 2022). One such epigenetic modification is N6-methyladenosine (m6 A), the most common and conserved internal transcript modification, which regulates various aspects of RNA fate, including nuclear trafficking, stability, alternative splicing, translation, and RNA–protein interaction (Boulias and Greer 2023). The m6 A modification is dynamically regulated by "writers" (installers), "erasers"(removers), and "readers"(recognizers), such as YT521-B homology (YTH) family proteins (YTHDF1/2/3 and YTHDC1/2) and insulin-like growth factor 2 mRNA-binding proteins (IGF2BP1/2/3) (Zaccara et al. 2019). Increasing evidence indicates that m6 A-binding proteins play critical roles in the progression of pediatric cancers, including neuroblastoma (NB), hepatoblastoma (HP), and acute myeloid leukemia (ALL) (Liu et al. 2022; Wang et al. 2024; Hong et al. 2023). However, the molecular mechanisms by which m6 A-binding proteins regulate their target genes to promote pediatric cancer progression remain poorly understood.

YTHDF1 (YTH N6-methyladenosine RNA binding protein 1), an m6 A reader protein, has been identified as a key regulator of RNA translation in

several adult cancers, but its role in pediatric cancers, especially in MRTK, has not been thoroughly studied(Bao et al. 2023; Liu et al. 2020; Ren et al. 2023). Additionally, the precise involvement of ferroptosis, a form of iron-dependent, non-apoptotic cell death driven by lipid peroxidation, remains unclear in the context of MRTK, although its known role in other pediatric malignancies like neuroblastoma and hepatoblastoma, and genes associated with ferroptosis hold a promise as therapeutic targets (Lu et al. 2021; Alborzinia et al. 2022; Zhang et al. 2023; Li et al. 2021). In particular, the precise role of ferroptosis in MRTK has not been fully elucidated.

Since our initial screening experiments identified that YTHDF1 expression was significantly upregulated in MRTK cells, suggesting its potential role in driving tumorigenic processes, we focused on YTHDF1 in this study. We first knocked out YTHDF1 by CRISPR/Cas and then characterized YTHDF1 KO clones. Through 4D label-free mass spectrometry (MS) analysis we identified GSTM2 as a potential target. Furthermore, YTHDF1 KO significantly sensitized MRTK cells to ferroptosis, a form of regulated cell death driven by iron-dependent lipid peroxidation, whereas overexpression of GSTM2 in YTHDF1 KO cells increased tolerance to ferroptosis, suggesting that GSTM2 plays a protective role in maintaining cellular homeostasis under oxidative stress conditions.

Materials and methods

Cell lines

293 T and HK-2 cells were obtained from Stem Cell Bank, Chinese Academy of Sciences and maintained in Dulbecco's Modified Eagle Medium (DMEM) (Coring, USA) supplemented with 10% fetal bovine serum (FBS, Coring, USA). G401 cells (provided by Professor Zhengyan Zhao, Children's Hospital, Zhejiang University, Hangzhou, China) were cultured in McCoy's 5 A Medium (Procell, China) supplemented with 10% FBS. All the medium contains 100 U/ml penicillin, and 100 mg/ml streptomycin. All cell lines were cultured at 37 °C in 5% CO2 incubator.

Construction of plasmids

For expression of GSTM2, we amplified from cDNA using primers GSTM2 –R1-5.1 and GSTM2–BamH1-3.1 (Table 1) and then cloned into pCDH-MSCV-MCS-EF1α-GFP +Puro expression vector (SBI system Bioscience, USA) by 2X MultiF Seamless Assembly Mix Kit (Abclonal, China). All DNA fragments for cloning purpose were amplified by chain polymerase reaction (PCR) with the high-fidelity Phusion enzyme (New England Biolabs, USA). All constructive plasmids were verified by DNA sequencing.

Lentivirus package and infection

Lentivirus was packaged in 293 T cells as previously described. Briefly, the lentiviral vector containing inserts of interest and three packaging system plasmid (Rev,Gag and VSVG) were mixed and transfected into 293 T cells with EndoFectin-Lenti reagent (GeneCopoeia, USA), and then the virus containing culture medium was collected 48 h after transfection and spun for 10 min at 3000 r.p.m. Lentivirus infection was carried out in 6-well plates by mixing 500 µl virus supernatant and 500 µl regular culture medium containing 0.8 µl polybrene (10 mg/ml).

YTHDF1 KO by CRISPR/Cas9 approach

DF1 KO in G401 cells was performed as previously described (Peng et al. 2023). Briefly, the lentiviral vector carrying Cas9 and dual gRNAs were introduced into G401 cells by infection. At 3 days after infection, cells were subject to puromycin selection.

Table 1 Primers used in this study

GSTM2-RT-5.3	TGTGCGGGGAATCAGAAAAGG
GSTM2-RT-3.3	GCTGGGCTCAAATACTTGGTTT
SLC7 A11-RT-5.1	ATGCAGTGGCAGTGACCTTT
SLC7 A11-RT-3.1	GGCAACAAAGATCGGAACTG
PRDX1-RT-5.1	TGGTTGAACCCCAAGCTGATA
PRDX1-RT-3.1	GTGGGGCACACAAAGGTGAA
GAPDH-5.1	GAGTCAACGGATTTGGTCGT
GAPDH-3.1	TTGATTTTGGAGGGATCTCG
U6-RT-5.1	TGCTCGCTTCGGCAGCACAT
U6-RT-3.1	ATATGGAACGCTTCACGAAT

Then 2 weeks later, individual colonies were manually collected and expanded in 24-well plates. KO clones were characterized by western blot.

Cell growth assay by CCK-8

CCK-8 assay was conducted to check the effect of DF1 KO or GSTM2 expression on cell growth. Briefly, G401 cells were seeded into 96-well plates at a density of 1×10^4 cells/well, and the measurement was performed at 24, 48, 72 h after seeding. The absorbance at 450 nm was determined using a microplate reader (TECAN, Spark, Switzerland).

Quantitative RT-PCR (qRT-PCR)

Total RNA was isolated by Direct-zol RNA Miniprep Kits (Zymo, USA). Real-time PCR was performed using SYBR Green kit (Vazyme, Q221) and specific primers on a Bio-Rad CFX Opus96 platform (Bio-Rad, Hercules, USA). All primers used are listed in Table 1. Delta-delta Ct values were used to determine their relative expression.

Cell migration and invasion assay

Cell migration and invasion assays were determined using 24-well transwell inserts or Matrigel transwell inserts from BD Biosciences (San Jose, CA, USA), respectively as previously described with modification. Briefly, 3×10^4 cells in 100 µl serum-free medium were added to the upper compartment of the chamber, while the lower compartment was filled with 600 µL of regular culture medium, then the cells were incubated at 37 °C for 36 h. Cells remaining on inside membrane surface in the upper chambers were removed with a cotton swab, whereas the cells on the lower surface were fixed in methanol for 10 min at room temperature, washed with PBS and stained with 0.5% crystal violet and counted as described previously (Gupta et al. 2014). The invasion assay was done by the same procedure with transwell inserts pre-coated with matrigel (Corning® BioCoat™, CLS354480, USA), and 5×10^4 tumor cells were added to the upper chamber.

Colony formation assay

For the colony formation assay, cells were seeded in 6-well plates. After 14 days, the cells were fixed with 4% PFA (Solarbio, Bejing) and then stained with 0.5% crystal violet. The number of colonies was countered for five representative fields. The experiments were repeated for three times.

Western blot

Cells were harvested, and proteins were extracted and quantified as previously described with some modification (Sachdeva et al. 2011). Briefly, cells were harvested and the cell pellets were washed with ice-cold phosphate buffered saline (PBS). Next, the cells were lysed with RIPA buffer (Fdbio, China) and denatured with 5xSDS sample buffer or directly lysed by home-made 2xSDS sample buffer. Protein samples were separated using 10% or 12% SDS-PAGE before transferring to PVDF membrane. Membrane was then blocked by 5% BS in TBST at room temperature for 1 h and then incubated with primary antibodies overnight at 4 °C. After washed six times with TBST, the membrane was incubated with a secondary antibody labeled with either IRDye 800 CW or IRDye 680. Finally, signal intensity was determined using the Amersham Typhoon NIR System.

Quantitative proteomics analysis

The 4D-label-free-based quantitative proteomic analysis of G401 DF1 KO cells and vector controls cells was carried out by Jingjie PTM Biolabs Inc. (Hangzhou, China). Cell samples were sonicated, lysed, and centrifuged to obtain the supernatant and its protein concentration was measured. The tryptic peptides were dissolved in solvent A (0.1% formic acid, 2% acetonitrile/in water), directly loaded onto a home-made reversed-phase analytical column (25-cm length, 75/100 µm i.d.). Peptides were separated with a gradient from 6 to 24% solvent B (0.1% formic acid in acetonitrile) over 70 min, 24% to 35% in 14 min and climbing to 80% in 3 min then holding at 80% for the last 3 min, all at a constant flow rate of 450 nL/min on a nanoElute UHPLC system (Bruker Daltonics). The peptides were subjected to capillary source followed by the timsTOF Pro (Bruker Daltonics) mass spectrometry. The electrospray voltage applied was 1.60 kV. Precursors

and fragments were analyzed at the TOF detector, with a MS/MS scan range from 100 to 1700 m/z. The timsTOF Pro was operated in parallel accumulation serial fragmentation (PASEF) mode. Precursors with charge states 0 to 5 were selected for fragmentation, and 10 PASEF-MS/MS scans were acquired per cycle. The dynamic exclusion was set to 30 s.

The MS/MS data were analyzed using the MaxQuant search engine (version 1.6.15.0). Tandem mass spectra were matched against the human SwissProt database (20,422 entries), combined with a reverse decoy database. Trypsin/P was selected as the cleavage enzyme, allowing for up to two missed cleavages. The precursor ion mass tolerance was set to 20 ppm for the initial search and 5 ppm for the main search, while the fragment ion mass tolerance was set to 0.02 Da. Carbamidomethylation of cysteine was specified as a fixed modification, and acetylation at the protein N-terminus and oxidation of methionine were set as variable modifications. The false discovery rate (FDR) for protein and peptide identification was set to 1%.Then, Pearson's correlation coefficient, principal component analysis (PCA), and relative standard deviation were used to evaluate the repeatability of samples from each group. Differential proteins were obtained after the qualification of samples, whose differences in relative quantification in two groups were compared by T-test, and the corresponding p-value was calculated. In addition, with a criterion of p-value ≤ 0.05, the protein ratio > 1.5 was regarded as up-regulation, while the protein ratio $< 1/1.5$ as down-regulation.

Assessment of cytosolic ROS

Cells were seeded at 3×10^5 cells per well in 6-well plates. Next day, cells were incubated with 2',7'-dichlorofluorescin diacetate (DCFH-DA; 10 mM; Beyotime, S0033S) for 30 min at 37 °C in the dark. The fluorescence-labeled cells were visualized by an inverted fluorescence microscopy (Leica, DMi8, Germany), and number of fluorescent cells were analyzed by ImageJ software (11.27.42).

In silico analysis of the binding of YTHDF1 to GSTM2 m6 A site

The potential m6 A sites were predicted using the online tools SRAMP (http://www.cuilab.cn/sramp). CLIP-seq data of GSTM2 were extracted from the POSTAR3 database (http://postar.ncrnalab.org) (Zhao et al. 2022).

RNA immunoprecipitation (RIP) assay

G401 cells were grown in 10 cm dish to 90% confluency, and then washed twice with ice-cold PBS and scraped off in 1 mL PBS. Next the cells were centrifuged and re-suspended in 1 mL RIP lysis buffer (150 mM KCl, 25 mM Tris–HCl (pH 7.4), 5 mM EDTA, 0.5% NP-40, with 100 U/ml RNase inhibitor and protease inhibitor cocktail). After that, 5 µg DF1 antibody or negative control rabbit IgG (Boytime, China) was added to the cell lysates and incubated overnight at 4℃ with rotation. Next day, protein A/G PLUS-Agarose Beads (Santa Cruz, USA) were added to IP reaction and continued for another 2 h incubation. Beads were washed 4 times with NP-40 lysis buffer and then treated with proteinase K to remove proteins. Then interested RNAs were purified by TRIzol methods (ThermoFisher Scientific) and detected by qRT-PCR.

m6 A RNA immunoprecipitation (MeRIP) assay

The MeRIP assay was performed as previously described. Total RNA was isolated from a 10 cm dish G401 cells and dissolved in 50 µl RNase-free water, of which 5 µl was saved as RNA input and the remaining 45 µl RNA was added to 500 µl pulldown lysis buffer containing RNase inhibitor. The total RNA was mixed with mouse IgG or m6 A antibody. The tubes were then rotated overnight at 4 °C, followed by incubation with protein A/G beads under the same condition overnight. Finally, m6 A bound RNA was extracted with TRIzol, followed by RT-PCR as described above.

RNA stability assay

To measure the stability of GSTM2 mRNA, 2 µg/mL of actinomycin D (Selleck, USA) was used to treat G401 cells. The procedure of isolating total RNA for qPCR analysis was as described above. Finally, the mRNA level at the indicated time points was calculated and normalized using U6.

Statistical analysis

All data are expressed as the mean ± SD. Statistical analyses were performed with GraphPad Prism 10.1 software. The differences between two groups of data were analyzed by unpaired Student's t test, and differences among three or more groups were analyzed by one-way analysis of variance (ANOVA) or two-way ANOVA followed by a post hoc Tukey test. A value of $P < 0.05$ was considered statistically significant.

Results

YTHDF1 is highly expressed in MRTK cells and loss of YTHDF1 suppresses RTK cell progression

During screening for potential m6 A reader proteins in MRTK cells, we found that YTHDF1 was upregulated. Although YTHDF1 is a well-known m6 A reader protein that has been extensively studied and implicated in tumorigenesis regulation in adult cancers, it has not been adequately studied in childhood tumors, including MRTK. In this regard, we compared the protein expression of YTHDF1 among HK-2 (normal adult human kidney proximal tubule epithelial cell), 293 T (human embryonic kidney cell), and G401 (MRTK cells). Western blot revealed that YTHDF1 level was higher in G401 cells than in HK-2 and 293 T cells (Fig. 1A). To determine whether YTHDF1 plays a role in MRTK progression, we employed the CRISPR/Cas9 approach to knock out YTHDF1 in G401 cells. We obtained a number of single KO clones and chose three KO clones for further characterization (Fig. 1B). CCK-8 assays revealed that YTHDF1 KO decreased cell proliferation (Fig. 1C) and colony formation assays showed YTHDF1 KO suppressed cell survival (Fig. 1D and E). Furthermore, YTHDF1 KO suppressed cell migration and invasion in G401 cells (Figs. 1F-H). Taken together, these results suggest that YTHDF1 could play an important role in MRTK progression.

Knockout of YTHDF1 sensitizes MRTK cells to chemotherapy

To date, preoperative high-dose chemotherapy is still the first-line treatment for MRTK patients. The most commonly used regimen is the alternating use of vincristine, doxorubicin, carboplatin and actinomycin D. In order to explore whether YTHDF1 expression level impacts chemotherapy tolerance of MRTK cells, we treated YTHDF1 KO and vector control cells with doxorubicin at different concentrations (0.1, 0.25 and 0.5 μM). The cell survival rate was detected by CCK-8 assay after 48 h treatment. As shown in Fig. 1I, YTHDF1 KO significantly enhanced the sensitivity of G401 cells to doxorubicin, even at a relatively low concentration (0.1 μM). At 0.25 μM, ~50% of YTHDF1 KO cells survived after 48 h of treatment, as compared with vector control having more than 70% of the cells alive. Furthermore, we found that YTHDF1 KO sensitized the G401 cells to carboplatin and vincristine as well. At 20 μg/ml carboplatin, about 40% of vector control cells were alive, but only about 20% of cells were alive in the YTHDF1 KO group (Fig. 1J). Similarly, YTHDF1 KO G401 cells were also more sensitive to vincristine. At 10 nM of vincristine, about half of YTHDF1 KO cells were alive, but more than 70% of control cells remained alive (Fig. 1K). In summary, these results suggest that YTHDF1 could mediate response to chemotherapeutic drugs in MRTK cells.

Loss of YTHDF1 impairs glutathione metabolism associated signaling pathway and promotes ferroptosis of MRTK cells

YTHDF1 is a well-documented m6 A "reader" which actively promotes protein synthesis by interacting with translation machinery. We therefore examined the repertoire of protein expression change after YTHDF1 KO in G401 cells by 4D-Label-free quantitative proteomics (4D-LFQ). Depletion of YTHDF1 resulted in 88 up-regulated and 73 down-regulated proteins in KO clone #3, and 74 up-regulated and 60 down-regulated proteins in KO clone #27, compared with vector control cells (Fig. 2A). Among the differentially expressed genes, 32 were commonly altered in both KO clone #3 and KO clone #27 (Fig. 2B). Among the differentially expressed genes, 32 genes were altered both in KO clone #3 and #27. (Fig. 2B). Gene ontology (GO) molecular function analysis showed that several downregulated functions such as glutathione peroxidase activity, glutathione binding, and glutathione transferase activity in YTHDF1 KO group (Fig. 2C). A comprehensive heatmap showing

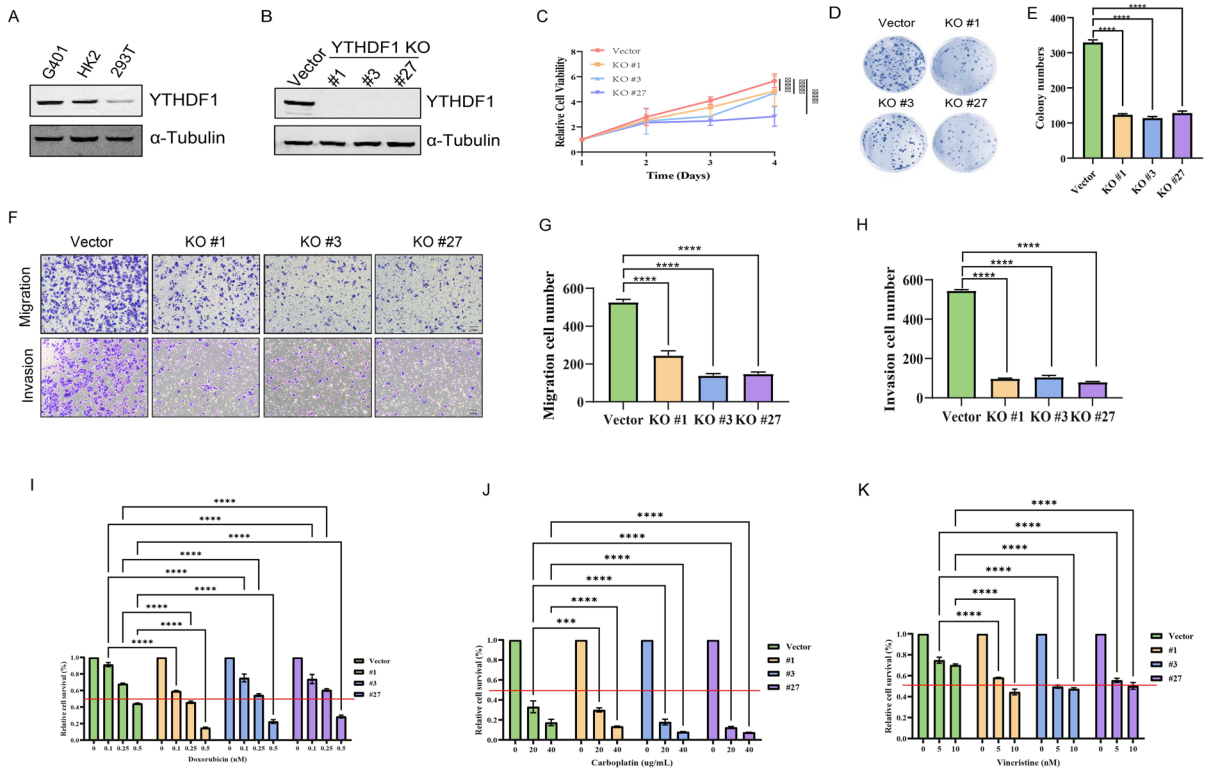

Fig. 1 YTHDF1 is upregulated in MRTKs and loss of YTHDF1 suppresses cell growth migration and chmeoresistance. (**A**) YTHDF1 expression levels in normal kidney cells and MRTK cells were assessed through western blot analysis. (**B**) YTHDF1 was knocked out in MRTK cells using CRISPR/Cas9, and YTHDF1 expression was confirmed by western blot. (**C**) CCK-8 assays were performed to determine cell growth after YTHDF1 KO in G401cells. (**D**) Colony formation assays of G401. (**E**) Quantification of colony formation assay results. (**F**) Knockout of YTHDF1 decreased the abilities of migration and invasion of MRTK cells. Scale bar, 100 μm. (**G**) Quantification of migration cells. (**H**) Quantification of invasion cells. CCK-8 assays were performed to examine the cell survival after different anticancer drug treatment at indicated concentrations. (**I**) YTHDF1 KO sensitizes MRTK cells to Doxorubicine. (**J**) YTHDF1 KO sensitizes MRTK cells to Carboplatin. (**K**) YTHDF1 KO sensitizes MRTK cells to Vincristine. Data are presented as Mean ± SD, $n = 3$. ***$P < 0.001$, ****$P < 0.0001$

significantly enriched molecular functions across the KO and Vector control. Several glutathione-related activities are consistently regulated (Fig. 2D). A bar graph displaying enriched protein domains based on PFAM analysis showed that Glutathione S-transferase N- and C-terminal domains were preferentially affected by YTHDF1 loss (Fig. 2E). The Kyoto Encyclopedia of Genes and Genomes (KEGG) and Protein domain analysis results also indicated that YTHDF1 deletion resulted in the disruption of glutathione (GSH) metabolism (Fig. 2F, G). GSH is an abundant antioxidant that maintains a redox balance in cells. Thus, tumor cells may develop various mechanism to protect them from oxidative stress, such as reactive oxygen species (ROS). Therefore, we explored the effects of YTHDF1 KO on ROS generation in MRTK cells. Deletion of YTHDF1 significantly increased lipid ROS generation (Fig. 2H and I). Since ferroptosis is linked to ROS and GSH regulation, we sought to determine whether YTHDF1 KO influence the ferroptosis of G401 cells. We treated YTHDF1 KO or vector control cells with ferroptosis inducer erastin at 1, 5 and 10 μM for 24 h, and then evaluated the cell viability by CCK-8 assay. We found that cell viability was significantly decreased by erastin treatment in YTHDF1 KO cells (Fig. 2J). Together, these findings suggest that deletion of YTHDF1 may impair glutathione metabolism and then exacerbate ferroptosis in MRTK cells.

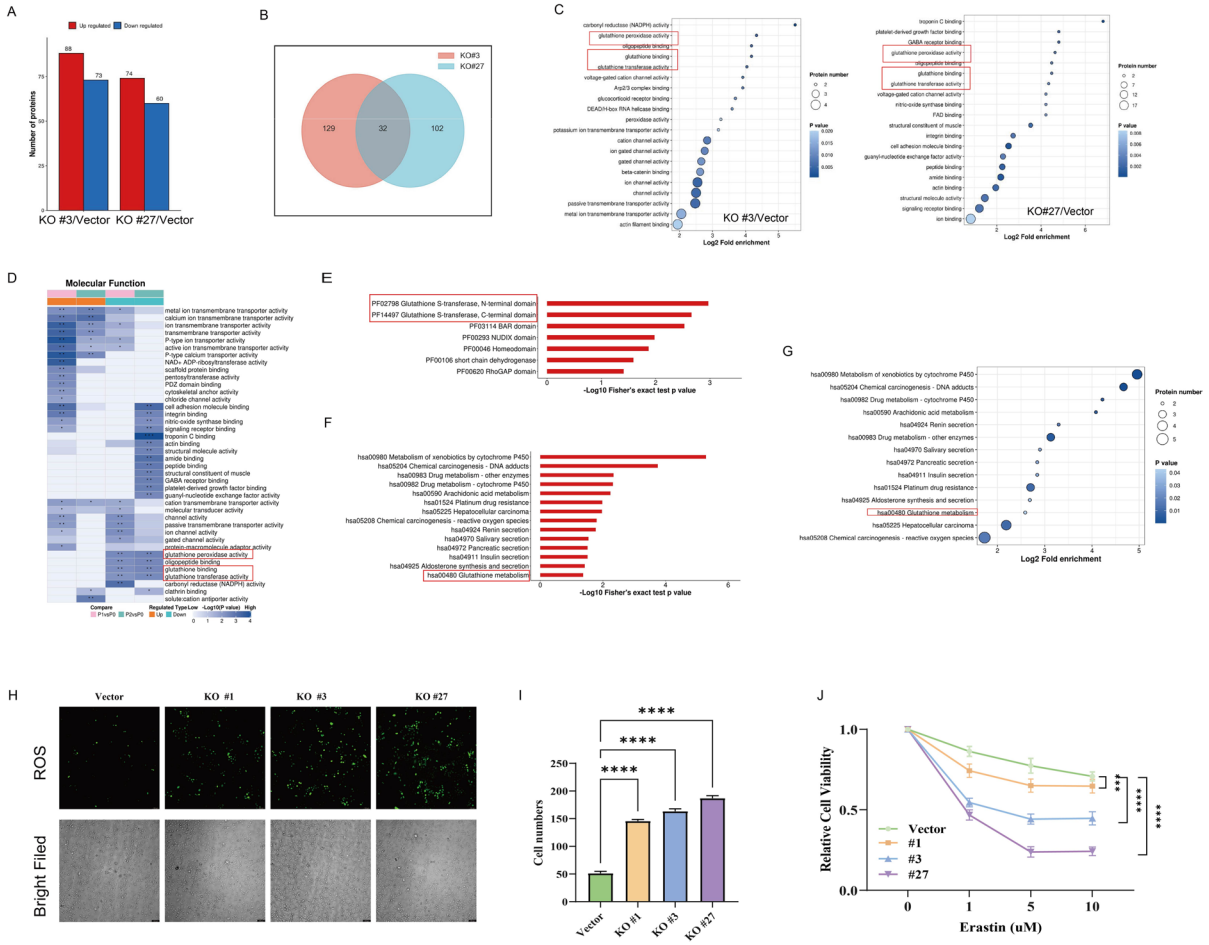

Fig. 2 Identification of the YTHDF1 targets in MRTK cells. (**A**) Chart of differentially expressed proteins identified by 4D-LFQ. (**B**) Venn diagram showing the differentially expressed proteins in two YTHDF1 KO clones. (**C**) KEGG enrichment analysis of differentially expressed proteins. (**D**) Cluster analysis results of GO annotations of the differentially expressed proteins. P0, protein from vector control cells; P1, protein from YTHDF1 KO#3; P2, protein from YTHDF1 KO#27. (**E**) Barplot map of downregulated protein domain by PFAM analysis. (**F**) Barplot map of KEGG enrichment analysis of the differentially expressed proteins. (**G**) Bulb map of KEGG enrichment analysis of overlapping differentially expressed proteins. (**H**) ROS positive cells as assessed by DCFH-DA fluorescence in YTHDF1 KO and vector control MRTK cells. The representative images obtained by a fluorescence microscope, scale bar, 100 μm. (**I**) Quantification of ROS positive cells. (**J**) CCK-8 assays were performed to detect the cell survival after erastin treatment. Data are presented as Mean ± SD, $*P < 0.05$, $**P < 0.01$, $***P < 0.001$, $****P < 0.0001$

GSTM2 is the target for YTHDF1

To investigate the downstream effectors through which YTHDF1 modulates glutathione metabolism, we conducted a comparative analysis of differentially expressed proteins shared between YTHDF1 KO#3 and KO#27 clones. As revealed by pathway enrichment analysis based on KEGG (Fig. 3A) and Reactome (Fig. 3B) databases, GSTM2 was identified as promising targets of YTHDF1. Indeed, the downregulation of GSTM2 (Fig. 3C) was further verified in YTHDF1-deficient G401 cells. Since YTHDF1 regulates target gene by recognizing m6 A modified sites, we next explored m6 A modification on GSTM2 mRNA through SRAMP ((Tomlinson et al. 2005). As shown in Fig. 3D, one m6 A modification site with high confidence were uncovered. Meanwhile, CLIP-seq data from the POSTAR3 (http://postar.ncrnalab.org) database also indicated the binding of GSTM2 to YTHDF1 (Fig. 3E). To

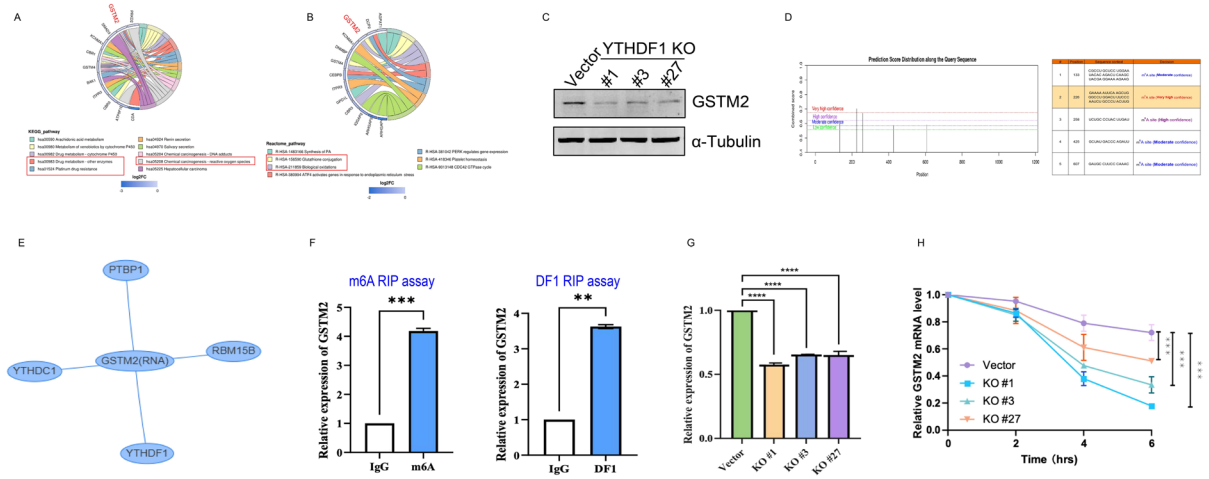

Fig. 3 m6a-modified GSTM2 is the target of YTHDF1 in MRTK cells. Circular chord diagrams illustrating the associations of GSTM2 with related genes and enriched pathways. (**A**) KEGG-based pathway enrichment analysis showing the involvement of GSTM2 and associated genes in metabolic and signaling pathways related to drug metabolism, detoxification, and carcinogenesis. (**B**) Reactome-based analysis further supporting the role of GSTM2 in redox regulation and xenobiotic response. (**C**) The protein level of GSTM2 in YTHDF1 KO and vector control cells. (**D**) Prediction of m6 A modification site on GSTM2 mRNA. (**E**) CLIP-seq data from POSTAR3 database indicates the binding of GSTM2 mRNA to YTHDF1. (**F**) RIP-qPCR detected the m6 A modification of GSTM2 mRNA,and the interaction between YTHDF1 and GSTM2. (**G**) GSTM2 mRNA level is downregulated in YTHDF1 KO cells. (**H**) YTHDF1 KO impairs the stability of GSTM2 mRNA. Data are presented as Mean ±SD,$^{**}P < 0.01$, $^{***}P < 0.001$

further verify that the m6 A modification of GSTM2 was recognized by YTHDF1, we performed m6 A RNA immunoprecipitation (MeRIP) assay and RNA immunoprecipitation (RIP), respectively. The MeRIP results showed that GSTM2 was obviously enriched by m6 A antibody (Fig. 3F, left panel). There was a about fourfold enrichment of GSTM2 by YTHDF1 antibody as compared to control IgG group (Fig. 3F, right panel). These results indicated that GSTM2 was subjected to m6 A modification, which was recognized by YTHDF1. It has been previously demonstrated that YTHDF1 not only directly initiates cap-independent translation but also enhances target RNA stability. We next checked the mRNA level of GSTM2 in YTHDF1 KO cells. Interestingly, we found the mRNA level of GSTM2 was downregulated upon YTHDF1 deletion as well (Fig. 3G), suggesting that YTHDF1 could regulate GSTM2 mRNA stability. To test this hypothesis, we treated YTHDF1 KO and vector control cells with RNA *de nove* synthesis inhibitor actinomycin D at various time points. Evidently, the mRNA of GSTM2 was less stable in YTHDF1 KO cells (Fig. 3H), suggesting that YTHDF1 could bind to m6 A-modified GSTM2 and enhance its stability.

GSTM2 is critical for YTHDF1-mediated cell growth

It has been reported that GSTM2 not only plays an important role in anticancer drug resistance in adult cancers, but also regulates the apoptotic pathway to prevent non-alcoholic steatohepatitis (NASH)(Peng et al. 2021; Lan et al. 2022). However, the role of GSTM2 in MRTK remains elusive. To determine the effect of GSTM2 on cell growth in G401 cells, we established stable GSTM2 knockdown cell by specific shRNA (OriGene, USA). Western blot results indicated GSTM2 expression was successfully downregulated in shGSTM2 cells as compared to vector control (Fig. 4A). Next, we further characterized two stable lines of shGSTM2 cells. GSTM2 knockdown significantly suppressed cell viability, as measured by CCK-8 (Fig. 4B). To further confirm that GSTM2 is a downstream target for YTHDF1, we overexpressed GSTM2 in YTHDF1 KO cells (Fig. 4C). As expected, overexpression of GSTM2 obviously restored growth rate of YTHDF1 KO cells (Fig. 4D-F), suggesting that GSTM2 is an important target for YTHDF1-mediated signaling to maintain the cell viability of MRTK cells.

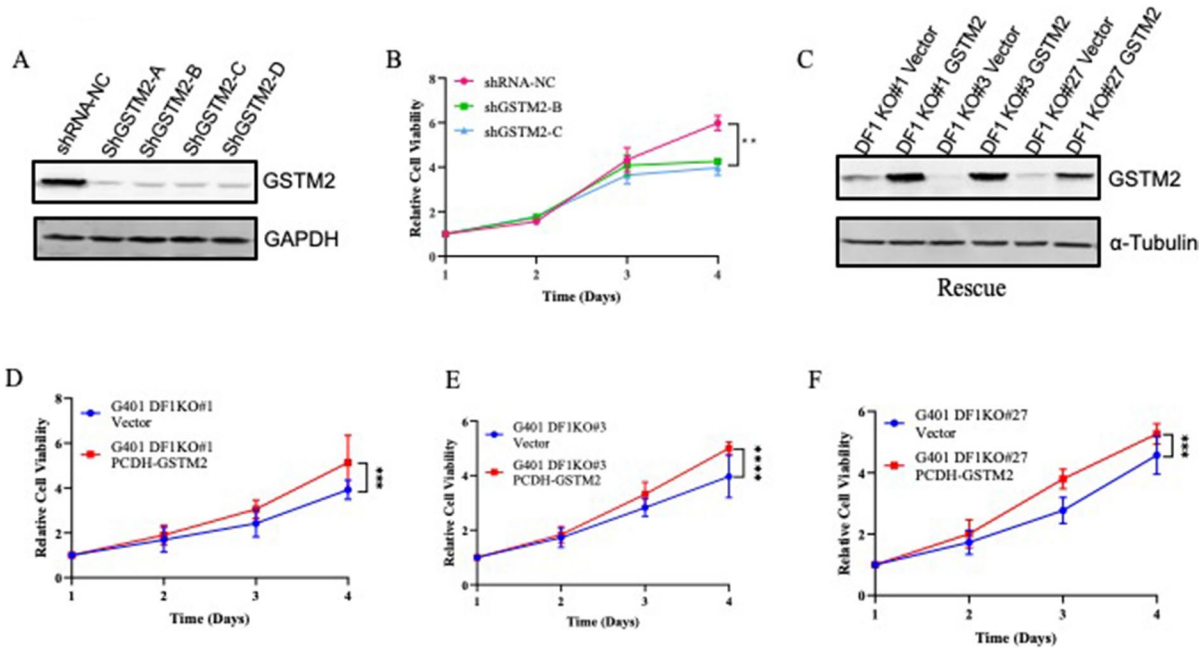

Fig. 4 GSTM2 contributes to the YTHDF1-mediated cell growth of MRTK cells. (**A**) GSTM2 was depleted in MRTK cells by shRNA. (**B**) The suppression of cell viability by GSTM2 knockdown was examined by CCK-8 assays. (**C**) Overexpression of GSTM2 in YTHDF1 KO cells. (**D**-**F**) CCK-8 results indicated overexpression of GSTM2 in YTHDF1 KO cells increases cell growth rate. Data are presented as Mean ± SD,*$P < 0.05$, **$P < 0.01$

YTHDF1/GSTM2 axis sensitizes MRTK cells to ferroptosis in a GPX4-indpendent manner

As shown above, YTHDF1 knockdown sensitized G401 cells to erastin-induced ferroptosis, and GSTM2 was identified as a critical target of YTHDF1. Therefore, we investigated whether GSTM2 knockdown could similarly increase sensitivity to erastin in G401 cells. As expected, GSTM2 knockdown increased the sensitivity to erastin-induced ferroptosis (Fig. 5A). Given the role of glutathione peroxidase 4 (GPX4) as a key regulator against ferroptosis, we next examined GPX4 expression in GSTM2 knockdown cells. Interestingly, GSTM2 knockdown did not alter GPX4 expression (Fig. 5B). Similarly, YTHDF1 KO had no effect on GPX4 expression (Fig. 5C). Additionally, neither GSTM2 knockdown nor YTHDF1 KO had any significant impact on the expression of the cystine/glutamate transporter SLC7 A11 (Fig. 5D, E). However, we found that peroxiredoxin 1 (PRDX1), a GPX-like antioxidant enzyme involved in peroxide reduction, was reduced in GSTM2 knockdown cells (Fig. 5F, G). Together these results suggest that the YTHDF1/GSTM2 axis plays a crucial role in regulating ferroptosis in MRTK cells. Although GPX4 is the main defense mechanism against ferroptosis, GSTM2 could function in parallel or complementary pathways.

Discussion

Malignant rhabdoid tumor of the kidney is the most aggressive childhood renal tumor with overall survival (OS) rates ranging from 22 to 42%, however, the underlying mechanisms of MRTK development are still elusive (Tomlinson et al. 2005). In this study, we identified that YTHDF1 upregulated in MRTK cells. Using KO approach in MRTK cell lines, we demonstrated that YTHDF1 plays an important role in MRTK progression, where YTHDF1 KO suppresses tumor cell growth, migration, invasion, and chemo-resistance, and furthermore, it increases susceptibility to ferroptosis. 4D label-free proteomics analysis revealed the glutathione metabolism pathway as a critical axis disrupted by YTHDF1 depletion. In

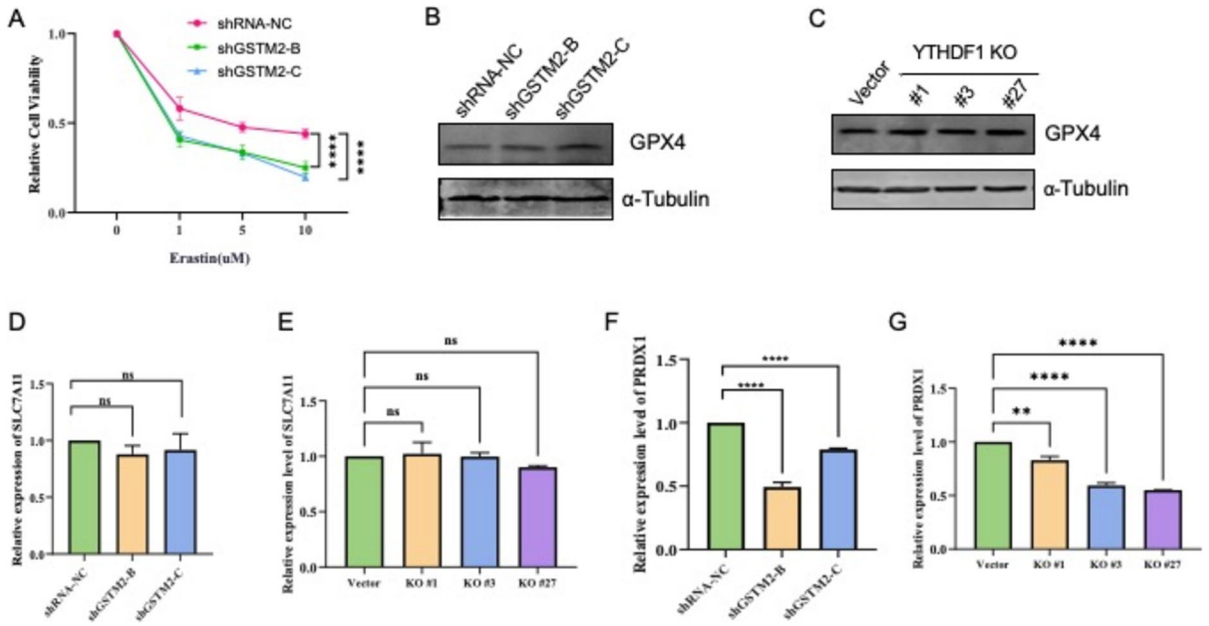

Fig. 5 GSTM2 is involved in YTHDF1-mediated ferroptosis. (**A**) Knockdown of GSTM2 sensitized MRTK cells to erastin treatment. (**B**) Knockdown of GSTM2 has no obvious effect on GPX4 expression. (**C**) Deletion of YTHDF1 has no effect on GPX4 expression. (**D**) Knockdown of GSTM2 does not affect the mRNA levels of SLC7 A11. (**E**) The KO of YTHDF1 does not alter the mRNA levels of SLC7 A11. (**F**) Knockdown of GSTM2 results in decreased the expression of PRDX1. (**G**) The KO of YTHDF1 similarly leads to a reduction in PRDX1 expression. Data are presented as Mean ± SD, ns, no significant, $*P < 0.05$, $**P < 0.01$, $***P < 0.001$, $****P < 0.0001$

particular, GSTM2 could serve as a key downstream target of YTHDF1 in MRTK cells. These findings suggest that GSTM2 could mediate the pro-tumorigenic functions of YTHDF1 in MRTK cells by enhancing cell survival and resistance to ferroptosis through modulation of the glutathione metabolism pathway.

As the most abundant chemically modification in mRNA, N6-methyladenosine (m6 A), plays a critical role in various biological functions, and large numbers of studies have provided links between dysregulated m6 A modification and cancer development, including pediatric cancer (Liu et al. 2022; Chen et al. 2022). The functions of m6 A are primarily executed by reader proteins, which recognize and bind to m6 A-modified RNA to mediate various downstream effects on RNA metabolism. YTHDF1, a member of the YTH domain family, has been implicated in many aspects of adult cancer development. The primary role of YTHDF1 is to promote translation efficiency of m6 A-modified mRNAs. After recognizing and binding to m6 A sites on mRNA, especially on 3'-UTR, YTHDF1 recruits the translation initiation machinery to the mRNA, thereby facilitating its efficient translation into proteins. While YTHDF1 primarily promotes translation, its role in RNA stability is more complex. In this study, we observed that YTHDF1 binds to m6 A-modified GSTM2 mRNA, and YTHDF1 KO impairs GSTM2 mRNA stability, leading to a decrease in its levels. A possible mechanism may involve shielding of GSTM2 mRNA from degradation while facilitating its translation.

Ferroptosis is a distinct form of programmed cell death characterized by iron (Fe^{2+})-dependent lipid peroxidation. Unlike apoptosis and necroptosis, ferroptosis is triggered by the accumulation of iron and the subsequent peroxidation of lipids, particularly within cellular membranes. Glutathione (GSH) is a tripeptide consisting of glutamate, cysteine, and glycine, and serves as a key antioxidant within cells. GSH is also essential for several detoxification processes and serves as a cofactor for various enzymes, including glutathione peroxidases (GPXs) (Boysen 2017). As the only enzyme capable of

reducing esterified oxidized fatty acids and cholesterol hydroperoxides, GPX4 has been identified as a major defense mechanism against ferroptosis. Nevertheless, GPX4-independent defense mechanisms have also been identified, including ferroptosis suppressor protein 1 (FSP1) and dihydroorotate dehydrogenase (DHODH)-regulated ferroptosis (Ma et al. 2022). These findings emphasize the intricate complexity of ferroptosis regulatory networks. The glutathione S-transferase (GST) family is a group of enzymes that play a key role in cellular detoxification. By catalyzing the conjugation of the antioxidant GSH to various electrophilic compounds, the GSTs protects cells from oxidative stress and damage caused by ROS and toxic chemicals. It has been demonstrated that GSTP1, a member of the GST family, protects cells from ferroptosis by catalyzing the conjugation of GSH to 4-hydroxynonenal (4-HNE) through its selenium-independent GSH peroxidase activity (Zhang, et al. 2023). GSTM2 plays a central role in phase II detoxification by catalyzing the conjugation of GSH to harmful substances such as drugs, carcinogens, and products of lipid peroxidation. Beyond detoxification, GSTM2 has been implicated in regulating cell signaling pathways related to stress response, inflammation, and apoptosis. It may act as a modulator in pathways triggered by oxidative damage and other stresses, contributing to cell survival and adaptation (Peng et al. 2021; Lan et al. 2022; Li et al. 2022). In the present study, GSTM2 was identified as a target of YTHDF1 through m6 A modification on its mRNA. The downregulation of GSTM2 resulting from YTHDF1 deletion inhibits MRTK progression in vitro. Thus, the YTHDF1/GSTM2 axis protects MRTK cells against ferroptosis. We speculate that this protective mechanism may operate independently of the canonical SLC7 A11/GPX4 pathway, suggesting the involvement of alternative regulatory processes in ferroptosis resistance.

Conclusions

We identified that YTHDF1 plays oncogenic role in MRTK cells that regulates glutathione metabolism by regulating GSTM2 expression. Specifically, GSTM2 is likely to function through detoxification and antioxidant defense, protecting MRTK cells from chemotherapy and drug-induced ferroptosis. Therefore, targeting the YTHDF1/GSTM2 axis could represent a promising therapeutic strategy for the treatment of MRTK.

Acknowledgements We would like to thank Dr. Zhengyan Zhao for the gift of the G401 cell line.

Author contributions Qian-Wen Xiong, Yuntao Liu and Min He carried out most of the experiments; Xiao-Die Shen performed YTHDF1 KO cell line identification; Manli Zhao and Shuang-ai Liu analyzed quantitative proteomics analysis results; Jinhu Wang and Wan-Xin Peng designed the project; Jinhu Wang revised the section of clinical background of MRTK; Wan-Xin Peng supervised all the analysis and revised the manuscript. All authors read and approved the final version of the manuscript.

Funding This research was supported by grants from National Natural Science Foundation of China (No. 82072703, WP) and the Key project of Huadong Medicine Joint Funds of the Zhejiang Provincial Natural Science Foundation of China (No. LHDMZ23H160005, WP).

Data availability No datasets were generated or analysed during the current study.

Declarations

Conflict of interests The authors declare no competing interests.

References

Alborzinia H, et al. MYCN mediates cysteine addiction and sensitizes neuroblastoma to ferroptosis. Nat Cancer. 2022;3(4):471–85.

Bao Y, et al. Targeting m(6)A reader YTHDF1 augments antitumour immunity and boosts anti-PD-1 efficacy in colorectal cancer. Gut. 2023;72(8):1497–509.
Boulias K, Greer EL. Biological roles of adenine methylation in RNA. Nat Rev Genet. 2023;24(3):143–60.
Boysen G. The glutathione conundrum: stoichiometric disconnect between its formation and oxidative stress. Chem Res Toxicol. 2017;30(5):1113–6.
Chen Y, et al. The role of m6A modification in pediatric cancer. Biochim Biophys Acta Rev Cancer. 2022;1877(2):188691.
Cheng H, et al. Clinical and prognostic characteristics of 53 cases of extracranial malignant rhabdoid tumor in children. A single-institute experience from 2007 to 2017. Oncologist. 2019;24(7):e551–8.
Gupta SC, et al. Acidosis promotes invasiveness of breast cancer cells through ROS-AKT-NF-kappaB pathway. Oncotarget. 2014;5(23):12070–82.
Hanahan D. Hallmarks of cancer: New dimensions. Cancer Discov. 2022;12(1):31–46.
Hong YG, et al. The RNA m6A reader YTHDF1 is required for acute myeloid leukemia progression. Cancer Res. 2023;83(6):845–60.
Koh KN, et al. Epidemiologic and clinical outcomes of pediatric renal tumors in Korea: a retrospective analysis of the Korean pediatric hematology and oncology group (KPHOG) data. Cancer Res Treat. 2023;55(1):279–90.
Lan T, et al. Hepatocyte glutathione S-transferase mu 2 prevents non-alcoholic steatohepatitis by suppressing ASK1 signaling. J Hepatol. 2022;76(2):407–19.
Li JX, et al. Down-regulation of activating transcription factor 3 (ATF3) in hepatoblastoma and its relationship with ferroptosis. Int J Gen Med. 2021;14:9401–18.
Li C, et al. GSTM2 is a key molecular determinant of resistance to SG-ARIs. Oncogene. 2022;41(40):4498–511.
Liu T, et al. The m6A reader YTHDF1 promotes ovarian cancer progression via augmenting EIF3C translation. Nucleic Acids Res. 2020;48(7):3816–31.
Liu L, et al. The N6-methyladenosine modification enhances ferroptosis resistance through inhibiting SLC7A11 mRNA deadenylation in hepatoblastoma. Clin Transl Med. 2022;12(5):e778.
Liu J, et al. BKM120 inhibits malignant rhabdoid tumor of the kidney through induction of apoptosis and G0/G1 phase arrest. Eur J Pharmacol. 2023;951:175747.
Lu Y, et al. MYCN mediates TFRC-dependent ferroptosis and reveals vulnerabilities in neuroblastoma. Cell Death Dis. 2021;12(6):511.
Ma T, et al. GPX4-independent ferroptosis-a new strategy in disease's therapy. Cell Death Discov. 2022;8(1):434.
Peng L, et al. Downregulation of GSTM2 enhances gemcitabine chemosensitivity of pancreatic cancer in vitro and in vivo. Pancreatology. 2021;21(1):115–23.
Peng WX, et al. N6-methyladenosine modified LINC00901 promotes pancreatic cancer progression through IGF2BP2/MYC axis. Genes Dis. 2023;10(2):554–67.
Ren W, et al. The function and clinical implication of YTHDF1 in the human system development and cancer. Biomark Res. 2023;11(1):5.
Sachdeva M, et al. MicroRNA-101-mediated Akt activation and estrogen-independent growth. Oncogene. 2011;30(7):822–31.
Smith MJ, et al. SMARCB1 mutations in schwannomatosis and genotype correlations with rhabdoid tumors. Cancer Genet. 2014;207(9):373–8.
Tomlinson GE, et al. Rhabdoid tumor of the kidney in the National Wilms' Tumor Study: age at diagnosis as a prognostic factor. J Clin Oncol. 2005;23(30):7641–5.
Voglino C, et al. Malignant rhabdoid tumor of the small intestine in adults: a brief review of the literature and report of a case. Surg Today. 2015;45(7):924–8.
Wang J, et al. METTL14 promotes neuroblastoma formation by inhibiting YWHAH via an m6A-YTHDF1-dependent mechanism. Cell Death Discov. 2024;10(1):186.
Xie S, et al. Extracranial malignant rhabdoid tumors in children: High mortality even with the help of an aggressive clinical approach. Eur J Pediatr. 2024;183(2):557–67.
Zaccara S, Ries RJ, Jaffrey SR. Reading, writing and erasing mRNA methylation. Nat Rev Mol Cell Biol. 2019;20(10):608–24.
Zhang L, et al. Ferroptosis regulator NOS2 is closely associated with the prognosis and cell malignant behaviors of hepatoblastoma: A bioinformatic and in vitro study. Front Oncol. 2023;13:1228199.
Zhang W, et al. SMURF2 predisposes cancer cell toward ferroptosis in GPX4-independent manners by promoting GSTP1 degradation. Mol Cell. 2023;83(23):4352-4369.e8.
Zhao W, et al. POSTAR3: an updated platform for exploring post-transcriptional regulation coordinated by RNA-binding proteins. Nucleic Acids Res. 2022;50(D1):D287–94.